

# Fluctuating Elastic Filaments Under Distributed Loads

Tianxiang Su\* and Prashant K. Purohit\*,<sup>†</sup>

**Abstract:** Filaments under distributed loads are common in biological systems. In this paper, we study the thermo-mechanical properties of an extensible thermally fluctuating elastic filament under distributed forces. The ground state of the filament is solved first, followed by an investigation of the thermal fluctuations around the ground state. We first consider a special case where the tangential component of the distributed force  $\tau$  is uniform along the filament. For the force-extension relation in this case, we show that the filament is equivalent to one under end-to-end applied force  $F = \tau L_0/2$  where  $L_0$  is the length of the filament. To study the thermal fluctuations under more general distributed loadings, the filament is first discretized into segments, and its energy is approximated up to quadratic order. Then the partition function of the discretized filament, or chain, is evaluated using multi-dimensional Gaussian integrals, from which free energy and other properties of the filament are derived. We show that a filament under distributed loads suffers larger thermal fluctuations than one with the end loads of the same magnitude. We also show that our results for a discretized filament agree with continuum theory for a continuous rod. Finally, we give some applications of our ideas to the stretching and fluctuation of DNA in non-uniform microfluidic channels.

## 1 Introduction

The wormlike chain model, or the fluctuating elastic filament model, has been extensively used to describe the mechanical behavior of semi-flexible polymers like DNA, actin and other long macromolecules [1, 2, 3, 4]. In particular, its force-extension relation is usually fitted to the experimental data of stretched polymers to extract their mechanical properties like the bending and stretching moduli [2]. Some authors have also used the model to predict the transverse fluctuations of the polymers and compare the results with experiments and simulations [5, 6, 7]. To account for the new and detailed results obtained using sophisticated experimental

---

\* Department of Mechanical Engineering and Applied Mechanics, University of Pennsylvania, Philadelphia, PA 19104, USA.

<sup>†</sup> E-mail: purohit@seas.upenn.edu

techniques, the fluctuating rod model is being continuously improved and generalized. For example, as the length scale at which people probe the mechanics of the polymers becomes shorter and shorter, boundary conditions and heterogeneity of the filament can not be ignored. To account for these effects, we have recently generalized the classical wormlike chain model to study polymers with heterogeneous mechanical properties that are loaded under different boundary conditions [7].

Most of the studies so far consider only the behavior of a polymer under end-to-end applied forces and torques. The reason for this may be that the majority of force-extension measurements on macromolecules are carried out in optical tweezers, magnetic tweezers, or atomic force microscopes (AFM), all of which apply forces at the end of the polymer chains. But, there are many other cases where biological filaments are subjected to distributed loads. For example, DNA in a nanofluidic or microfluidic channel is subjected to distributed drag force applied by the surrounding fluid flow. Molecular motors exert point loads, which are a special case of distributed loads, to the long actin filaments in cells and muscles. Also, a uniformly charged polymer in a constant electric field behaves as if it is stretched by a force that varies along the contour. The behavior of a filament under such distributed loads is not well understood. In fact, if one simply uses an end-to-end force model to fit the extension data for a piece of DNA subjected to uniform flow, the fitted drag coefficient is much lower than the true measured value [8]. A few groups have tried to tackle this problem theoretically in recent years [11, 12, 13]. Some of these works relied on phenomenological arguments [11], while some solved the problem in the limit of a weak force field [12].

In this paper, we first calculate analytically the force-extension relation for a continuous filament under uniform distributed load. We show using Fourier series that under uniform tangential force per unit reference length  $\tau$  along the filament, it suffers the same extension as one under end-to-end force of magnitude  $F = \tau L_0/2$ , where  $L_0$  is the contour length. However, a Fourier analysis of this kind is easy to do only when  $\tau$  is uniform. To consider more general loadings, we use our theoretical framework [7] developed earlier to investigate the thermo-mechanical properties of a discretized filament. In particular, we first find the ground state, or the minimum energy state, for a filament under distributed loads. Then the thermal fluctuation around this ground state is studied using a statistical mechanical approach. In particular, the partition function is obtained analytically using multi-dimensional Gaussian integrals. Once we get the partition function, the free energy of the system is derived immediately, and the thermo-mechanical properties of the system are calculated by differentiating the free energy. This method is capable of reproducing the classical wormlike chain results [7]. Moreover, because of the discretization, it can easily deal with filaments with heterogeneous mechanical prop-

erties. Here, we apply this framework to study the fluctuation of a filament under distributed loads.

## 2 Theory

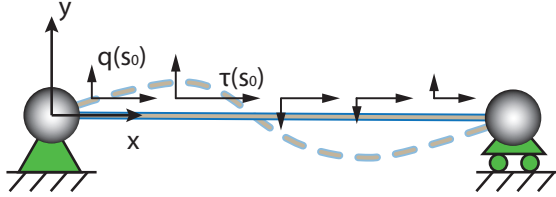


Figure 1: A fluctuating elastic filament (extensible wormlike chain) under distributed forces. The origin of the  $x - y$  coordinate system is set at the head of the filament, which is hinged. The other end of the filament is constrained to move only in the  $x$  direction. One possible deformed configuration of the filament is shown in dashed line.

### 2.1 Theory for a continuous elastic filament

Consider a semi-flexible polymer, or fluctuating elastic filament with stretching modulus  $K_s$  and bending modulus  $K_b$ . One end of the filament is hinged at the origin of the  $x - y$  coordinate system shown in Fig. 1, while the other end is constrained to move only in the  $x$ -direction. The reference configuration of the filament (the state under zero loads at zero temperature) is straight, lying on the  $x$  axis. The coordinate of its center line is  $[x, y] = [s_0, 0]$ . Here  $s_0$  is the reference arc length with  $s_0 \in [0, L_0]$ , and  $L_0$  being the undeformed contour length. Under distributed tangential force  $\tau(s_0)$  per unit reference length and distributed normal force  $q(s_0)$  per unit reference length, the filament deforms into  $[x, y] = [s_0 + u, w]$ , where  $u(s_0)$  and  $w(s_0)$  are the tangential and normal displacements respectively. Axial strain develops in the deformed filament and it can be expressed in terms of the displacements  $u(s_0)$  and  $w(s_0)$  assuming moderate rotations as:

$$\varepsilon(s_0) = \frac{ds - ds_0}{ds_0} \approx \frac{\partial u}{\partial s_0} + \frac{1}{2} \left( \frac{\partial w}{\partial s_0} \right)^2. \quad (1)$$

Here  $ds$  is the infinitesimal deformed arc length, and we keep terms up to the order of  $O(u, w^2)$  in the approximation.

The energy of the deformed filament, as a sum of its stretching, bending, and potential energies, is:

$$E = \int_0^{L_0} \frac{K_s}{2} \varepsilon^2 ds_0 + \int_0^{L_0} \frac{K_b}{2} \left( \frac{\partial^2 w}{\partial s_0^2} \right)^2 ds_0 - \int_0^{L_0} \tau u ds_0 - \int_0^{L_0} q w ds_0, \quad (2)$$

where  $K_s$  and  $K_b$  are the stretching and bending moduli of the filament. They are not necessarily constants and can be functions of the arc length  $s_0$  in the reference configuration. As discussed by Odijk [3], rather than express the energies in terms of the displacements  $u(s_0)$  and  $w(s_0)$ , it is more convenient to use  $\varepsilon(s_0)$  and  $w(s_0)$  as independent variables, because the total energy can be decoupled using these two variables. This is true even when the filament is under distributed loads. Using Eq. 1,  $u(s_0)$  in Eq. 2 can be eliminated and the energy can be grouped into two decoupled terms – one involving  $\varepsilon(s_0)$  only, and the other involving  $w(s_0)$  only:

$$E = E_\varepsilon + E_w, \quad (3)$$

where the expressions for the two energy terms are:

$$E_\varepsilon = \int_0^{L_0} \left[ \frac{K_s}{2} \varepsilon^2 - \tau \int_0^{s_0} \varepsilon ds_0 \right] ds_0, \quad (4)$$

$$E_w = \int_0^{L_0} \left[ \frac{K_b}{2} \left( \frac{\partial^2 w}{\partial s_0^2} \right)^2 + \frac{\tau}{2} \int_0^{s_0} \left( \frac{\partial w}{\partial s_0} \right)^2 ds_0 - qw \right] ds_0. \quad (5)$$

The minimum energy configuration can be evaluated by setting the variations  $\delta E_\varepsilon = 0$  and  $\delta E_w = 0$ . The former variation gives the strain of the minimum energy configuration:

$$\varepsilon_{\min}(s_0) = \frac{1}{K_s} \int_{s_0}^{L_0} \tau(s_0) ds_0, \quad (6)$$

while the latter variation yields a 4th order ODE for the transverse displacement  $w_{\min}(s_0)$  of the minimum energy configuration:

$$(K_b w''_{\min})'' - \left( w'_{\min} \cdot \int_{s_0}^{L_0} \tau ds_0 \right)' - q = 0, \quad (7)$$

with hinged-hinged boundary conditions  $w(0) = w'(0) = w(L_0) = w'(L_0) = 0$ . Here we use  $'$  to denote the derivative  $d/ds_0$ . We note again that in deriving these results, we do not assume the moduli  $K_s$  and  $K_b$  to be uniform. They can vary along the filament. By specifying the distributed loads  $\tau(s_0)$  and  $q(s_0)$ , we can

solve Eq. 6 and Eq. 7 to get  $\epsilon_{\min}$  and  $w_{\min}$  respectively. Then by using Eq. 1, we can obtain the longitudinal displacement  $u_{\min}$ . Thus, the deformed configuration of the filament, without taking thermal fluctuations into account, is known. This minimum energy configuration is the ground state of the filament around which the system is fluctuating.

While the partition function and fluctuations of a discrete semi-flexible chain can be evaluated under rather general loading conditions, which we will discuss in the next section, it is difficult to compute the same quantities analytically for a continuous filament unless the distributed load is uniform. Here we briefly discuss how one can evaluate the average end-to-end extension of a continuous filament under constant  $\tau$ , by using a Taylor expansion of the path integral [9], and the Fourier series method [2, 10] respectively for the small and large  $\tau$  limits. For simplicity, we also set the normal distributed force  $q = 0$  for now.

In the small  $\tau$  limit, the potential energy term involving  $\tau$  in the Boltzmann factor can be expanded using  $\exp(x) \approx 1 + x$ . After carrying out this exercise the Boltzmann weighted average end-to-end extension reads:

$$\langle \Delta x \rangle = \frac{1}{Z} \int x(L_0) \cdot \exp\left(-\frac{E_b + E_s - \tau \int_0^s x ds_0}{k_B T}\right) \mathcal{D}\vec{r} \tag{8}$$

$$= \beta \tau \left\langle \int_0^s x(s_0) \cdot x(L_0) ds_0 \right\rangle_0 + O(\tau^2), \tag{9}$$

where  $Z$  is the partition function,  $\beta = 1/k_B T$ ,  $E_b$  and  $E_s$  are the bending and stretching energies respectively. The key step here is that, after the expansion, the potential energy part in the Boltzmann factor is factored out and so the average  $\langle \cdot \rangle_0$  in Eq. 9 is evaluated in a  $\tau = 0$  ensemble.

Now, the problem in the small  $\tau$  limit is how to do the average in a  $\tau = 0$  ensemble. To solve this problem, we recall that for a wormlike chain in a  $\tau = 0$  ensemble, the correlation of its tangent angle  $\theta$  satisfies:  $\langle \theta(s) \cdot \theta(s') \rangle = \exp(-|s - s'|/\xi_p)$  [9], which can be used to evaluate  $\langle \int_0^s x(s_0) \cdot x(L_0) ds_0 \rangle_0$  in Eq. 9, given  $x(s_0) = \int_0^{s_0} \cos \theta ds_0$ . Here  $\xi_p$  is the persistence length of the wormlike chain. The calculation is tedious but the final result for  $\langle \Delta x \rangle$  turns out to be linear, as expected, in the small  $\tau$  limit:

$$\langle \Delta x \rangle = \frac{2\xi_p L_0}{Dk_B T} \left[ 1 - \frac{\xi_p}{L_0} \left( 1 - e^{-L_0/\xi_p} \right) \right] \cdot \frac{\tau L_0}{2} + \frac{\tau L_0^2}{2K_s}, \tag{10}$$

with  $D$  being the dimension of space, i.e.,  $D = 2, 3$  for a 2D and 3D chain respectively. The last term in the above equation is the contribution of the pure stretching term in the energy.

When  $L_0 \gg \xi_p$ , the force-extension relation is simply:

$$\langle \Delta x \rangle = \frac{2\xi_p L_0}{Dk_B T} \cdot \frac{\tau L_0}{2} + \frac{\tau L_0^2}{2K_s}. \quad (11)$$

One may recognize that the force-extension relation shown here for a filament under small uniform  $\tau$  is in exactly the same form as the relation for a filament under small end-to-end force  $F$ , with  $F$  being replaced by  $\tau L_0/2$ . Therefore, we conclude that, as far as the force-extension relation is concerned, at small loads a uniformly distributed tangential force is equivalent to an end-to-end force  $F_{\text{eff}} = \tau L_0/2$ .

In the large  $\tau$  limit, on the other hand, where the approximation of the tangent angle  $\theta \ll 1$  holds, one can use the Fourier series method to tackle the problem. As usual, we expand the tangent angle  $\theta = \partial w / \partial s_0$  in a Fourier cosine series:

$$\theta(s_0) = \sum_{n=1}^{+\infty} a_n \cos\left(\frac{2n\pi s_0}{L_0}\right). \quad (12)$$

There is no  $a_0$  term here because the hinged-hinged boundary condition requires  $\int_0^{L_0} \theta ds_0 = 0$ . Plugging the Fourier series into Eq. 5, the energy of the filament contributed by  $w$  becomes:

$$E_w = \sum_{n=1}^{+\infty} \left( \frac{K_b \pi^2 n^2}{L} + \frac{\tau L^2}{8} \right) a_n^2. \quad (13)$$

The equipartition theorem of statistical mechanics states that each quadratic mode should have an average energy equal to  $k_B T/2$ , which leads to:

$$\langle a_n^2 \rangle = \frac{k_B T}{2 \left( \frac{K_b \pi^2 n^2}{L} + \frac{\tau L^2}{8} \right)}, \quad (14)$$

Using Parseval's theorem, we obtain the expression for  $\int_0^{L_0} \langle \theta^2 \rangle ds_0$  from Eq. 14, which finally leads to the force-extension relation of a chain under uniform  $\tau$ :

$$\langle \Delta x \rangle = L_0 - \frac{k_B T L_0}{4\sqrt{K_b \tau L_0/2}} \left[ \coth\left(L_0 \sqrt{\frac{\tau L_0}{2K_b}}\right) - \frac{1}{L_0} \sqrt{\frac{2K_b}{\tau L_0}} \right] + \frac{\tau L_0^2}{2K_s}. \quad (15)$$

Here again the last term is the independent contribution from the stretching energy  $E_\epsilon$ . Once again, we see that the force-extension relation, in the large  $\tau$  limit, has the same form as a wormlike chain under a large effective end-to-end force  $F_{\text{eff}} = \tau L_0/2$ . Hence, we have shown that this equivalent relation holds for both small and

large  $\tau$ . Following Marko and Siggia [2], the force-extension relation for a filament under uniform  $\tau$  can be written as:

$$\frac{\tau L \xi_p}{2k_B T} = \frac{1}{4} \left(1 - \frac{x}{L_0}\right)^{-2} - \frac{1}{4} + \frac{x}{L_0} - \frac{\tau L_0}{2K_s}. \quad (16)$$

From here on, we will focus on the large  $\tau$  limit only because the filament under small loads behaves as a linear entropic spring.

We saw in the above discussion that the Fourier series method works only when  $\tau$  is a constant. It is possible to deal with non-uniform distributed force if one ignores the boundary conditions and applies the wormlike-chain constitutive law to an infinitesimal segment on the continuous filament, and then integrates to recover the end-to-end extension of the entire filament. In particular, let  $f(s_0)$  be the *internal* force along the filament in the tangential direction. Balance of forces on an infinitesimal segment  $ds_0$  reads (Fig. 2A):

$$f(s_0 + ds_0) - f(s_0) + \tau ds_0 = 0, \quad (17)$$

which leads to  $\partial f / \partial s_0 = -\tau$ , whose solution with boundary condition  $f(L_0) = 0$  is:

$$f(s_0) = \int_{s_0}^{L_0} \tau(s_0) ds_0. \quad (18)$$

This tells us that, when  $\tau > 0$ , the internal stress decreases from the fixed end to the other end, which makes sense because  $\tau$  is positive when pointing away from the fixed end. On the other hand, the stretch  $\lambda(s_0) = \varepsilon(s_0) + 1$  for a 2D extensible wormlike chain is [3]:

$$\lambda = \frac{\partial x}{\partial s_0} = 1 - \frac{k_B T}{4\sqrt{K_b f}} \left[ \coth \left( L \sqrt{\frac{f}{K_b}} \right) - \frac{1}{L} \sqrt{\frac{K_b}{f}} \right] + \frac{f}{K_s}. \quad (19)$$

Plugging Eq. 18 into Eq. 19, eliminating  $f$  and solving the ODE for  $x(s_0)$ , we can obtain  $\Delta x = x(L_0) - x(0)$ . Note that this procedure works regardless of whether  $\tau$  is a constant. In particular, if  $\tau$  is uniform along the length of the filament, the result is:

$$\langle \Delta x \rangle = L_0 - \frac{k_B T}{2\tau L_0} \log \left[ \frac{\sinh \omega}{\omega} \right] + \frac{\tau L_0^2}{2K_s}, \quad (20)$$

where  $\omega = L\sqrt{\tau L_0/K_b}$ . Eq. 20 is not exactly the same as Eq. 15. This is because to derive Eq. 20, we have ignored the boundary condition that leads to the force-extension relation of a wormlike chain, and used it as the constitutive relation for

an infinitesimal segment. However, we will show later (Fig. 2B) that the force-extension curves from the two equations are close though not exactly the same.

The advantage of analyzing a continuous filament as we have done above is that we get analytic closed form results. However, as we have already seen, the analysis is either limited to special cases or relies on some additional assumptions that are not easy to verify. To get the exact thermal fluctuations of a filament under general distributed loads, it is convenient to first discretize it into segments. The partition function of the system, which is a path integral for a continuous filament, becomes a multi-dimensional Gaussian integral for a discretized filament or chain, and can be evaluated easily [14, 7]. In the limit where the discretized segment length  $l_0 \rightarrow 0$ , the number of discretized segments  $N \rightarrow +\infty$ , while  $L_0 = Nl_0$  is kept constant, the discrete chain becomes the desired continuous filament. Below, we discuss a discrete fluctuating filament under distributed forces.

## 2.2 Energy of a discretized elastic filament or semi-flexible chain

We use the following notations for a discrete chain.  $K_{si}$ ,  $K_{bi}$  are the stretching and bending moduli of segment  $i$  of the chain. They can be different for different  $i$ , and  $i \in [1, N]$ . The reference coordinate of the  $i$ th node of the chain is  $(x_i, y_i) = (il_0, 0)$ , so that the chain is straight lying on the  $x$  axis. Under distributed loads  $\tau_i$  and  $q_i$  per unit length on the  $i$ th segment, the node moves to  $(x_i, y_i) = (il_0 + u_i, w_i)$ , with  $(u_i, w_i)$  being the nodal displacements. The axial strain for each segment is represented by the vector  $\vec{\varepsilon}^T = [\varepsilon_1, \varepsilon_2, \dots, \varepsilon_N]$ . Furthermore, we define the discrete version of the tangent angle  $\theta(s_0) = dw/ds_0$  as follows:  $\theta_i = (w_i - w_{i-1})/l_0$ . We wish to write the energy of the discrete chain in terms of the strains  $\vec{\varepsilon}$  and the angles  $\vec{\theta} = [\theta_1, \dots, \theta_N]$ .

The discretized version of the energies (Eq. 4 and 5) are quadratic expressions which can be written compactly in matrix form. In particular, the discretized version of the energy term involving  $\varepsilon$  is (Eq. 4):

$$E_\varepsilon = \sum_{i=1}^N \left[ \frac{K_{si} l_0}{2} \varepsilon_i^2 - \tau_i l_0^2 \sum_{j=1}^i \varepsilon_j \right], \quad (21)$$

and it can be written compactly as:

$$E_\varepsilon = \frac{1}{2} \vec{\varepsilon}^T \cdot [\mathbf{K}_\varepsilon] \vec{\varepsilon} + \vec{R}_\varepsilon^T \cdot \vec{\varepsilon}, \quad (22)$$

with the  $N \times N$  stiffness matrix being  $[\mathbf{K}_\varepsilon]_{ij} = K_{si} l_0 \delta_{ij}$ , and the  $i$ th component of the vector  $\vec{R}_\varepsilon$  being  $-l_0^2 \sum_{j=i}^N \tau_j$ . Similarly, the energy term involving only  $w$  (Eq. 5)



can be written in terms of  $\vec{\theta}$ :

$$E_w = \sum_{i=1}^N \left[ \frac{K_{bi}}{2l_0} (\theta_i - \theta_{i-1})^2 + \frac{\tau_i l_0^2}{2} \sum_{j=1}^i \theta_j^2 - q_i l_0^2 \sum_{j=1}^i \theta_j \right] \quad (23)$$

$$= \frac{1}{2} \vec{\theta}^T \cdot [\mathbf{K}_\theta] \vec{\theta} + \vec{R}_\theta^T \cdot \vec{\theta}. \quad (24)$$

We note that the stiffness matrix  $[\mathbf{K}_\theta]$  is a sparse tridiagonal matrix.

Finally, to impose the boundary condition and to constrain the end of the chain such that  $w(L_0) = 0$ , we add a penalty energy:

$$E_p = \frac{K_p}{2} [w(L_0) - 0]^2 = \frac{K_p}{2} \left( \sum_{i=1}^N \theta_i l_0 \right)^2 \quad (25)$$

$$= \frac{1}{2} \vec{\theta}^T \cdot [\mathbf{K}_p] \vec{\theta}. \quad (26)$$

Eq. 24 and Eq. 26 can be combined, and therefore, we can write the total energy of the chain  $E = E_\varepsilon + E_w + E_p$  as:

$$E = \left\{ \frac{1}{2} \vec{\varepsilon}^T \cdot [\mathbf{K}_\varepsilon] \vec{\varepsilon} + \vec{R}_\varepsilon^T \cdot \vec{\varepsilon} \right\} + \left\{ \frac{1}{2} \vec{\theta}^T \cdot [\mathbf{K}_{\theta p}] \vec{\theta} + \vec{R}_\theta^T \cdot \vec{\theta} \right\}, \quad (27)$$

where  $[\mathbf{K}_{\theta p}] = [\mathbf{K}_\theta] + [\mathbf{K}_p]$ .

As for a continuous filament, the ground state of the discrete chain is computed first by solving  $\partial E / \partial \varepsilon_i = 0$  and  $\partial E / \partial \theta_i = 0$ . These result in two linear sets of equations:

$$[\mathbf{K}_\varepsilon] \vec{\varepsilon}_{\min} = -\vec{R}_\varepsilon, \quad [\mathbf{K}_{\theta p}] \vec{\theta}_{\min} = -\vec{R}_\theta, \quad (28)$$

which are solved to determine the ground state around which the chain fluctuates.

We next consider the thermal fluctuation around the ground state. We define the deviations from the ground state as  $\Delta \vec{\varepsilon} = \vec{\varepsilon} - \vec{\varepsilon}_{\min}$ ,  $\Delta \vec{\theta} = \vec{\theta} - \vec{\theta}_{\min}$ . Then the energy (Eq. 27) in terms of these deviation variables is simply:

$$E = E_{\min} + \frac{1}{2} \Delta \vec{\varepsilon}^T \cdot [\mathbf{K}_\varepsilon] \Delta \vec{\varepsilon} + \frac{1}{2} \Delta \vec{\theta}^T \cdot [\mathbf{K}_{\theta p}] \Delta \vec{\theta}, \quad (29)$$

where  $E_{\min}$  is the ground state energy. Note that the linear terms disappear when the energy is expressed in terms of the deviation variables.

### 2.3 Partition function and free energy

For a semi-flexible chain, the elastic and potential energies are usually comparable to the thermal energy  $k_B T$  at room temperature, where  $k_B$  is the Boltzmann constant and  $T$  is the temperature in Kelvin, set to be 300K in this study. Therefore, the chain does not stay in the ground state forever. Instead, it fluctuates and samples different configurations, labelled as  $\mathbf{v}$  below, around the ground state with Boltzmann statistics:  $P_{\mathbf{v}} \sim \exp(-E_{\mathbf{v}}/k_B T)$ . Here  $P_{\mathbf{v}}$  is the probability that a configuration  $\mathbf{v}$  with energy  $E_{\mathbf{v}}$  is sampled. The thermo-mechanical behavior of this fluctuating elastic chain can be evaluated using statistical mechanics by computing the partition function  $Z$ , which is the sum of Boltzmann factors over all the allowed configurations. In our case, the energy of the system has been written in a quadratic matrix form (Eq. 29) and the partition function is:

$$Z = \int_{-\infty}^{+\infty} \cdots \int_{-\infty}^{+\infty} \exp\left(-\frac{E}{k_B T}\right) d(\Delta\vec{\epsilon}) d(\Delta\vec{\theta}) \quad (30)$$

$$= e^{-\beta E_{\min}} \cdot \sqrt{\frac{(2\pi k_B T)^N}{\det[\mathbf{K}_{\epsilon}]}} \cdot \sqrt{\frac{(2\pi k_B T)^N}{\det[\mathbf{K}_{\theta p}]}} \quad (31)$$

where  $\beta = 1/k_B T$  and  $\mathbf{K}_{\epsilon}$  and  $\mathbf{K}_{\theta p}$  are  $N \times N$  matrices. From the partition function  $Z$ , we get the free energy  $G$  of the system:

$$G = -k_B T \log Z \quad (32)$$

$$= E_{\min} + \frac{k_B T}{2} \log \det[\mathbf{K}_{\epsilon}] + \frac{k_B T}{2} \log \det[\mathbf{K}_{\theta p}] - k_B T N \log(2\pi k_B T). \quad (33)$$

We note that  $G$  is the Gibbs free energy because the partition function (Eq. 31) is evaluated for a fixed temperature, fixed loads ensemble. Therefore, we have:

$$dG = -S \cdot dT - \sum_{i=1}^N u_i \cdot d(\tau_i l_0) - \sum_{i=1}^N w_i \cdot d(q_i l_0). \quad (34)$$

By differentiating the free energy we can get the thermo-mechanical properties, like the force-extension relation, of the chain.

### 2.4 Force-extension relation

Noticing that  $\tau_N l_0$  and  $u_N$  (distributed force on the last segment and longitudinal displacement of the last node) is a conjugate pair with respect to the energy (Eq. 34), we have:

$$\langle u_N \rangle = -\frac{\partial G}{\partial (\tau_N l_0)}. \quad (35)$$

In this paper,  $\langle \cdot \rangle$  denotes the usual ensemble average of all sampled configurations weighted by the Boltzmann factor. The average end-to-end extension of the chain is  $\langle \Delta x \rangle = \langle x(L_0) - x(0) \rangle = \langle x(L_0) \rangle = L_0 + \langle u_N \rangle$ , which turns out to be:

$$\langle \Delta x \rangle = \Delta x_{\min} - \frac{k_B T}{2l_0} \cdot \frac{\partial}{\partial \tau_N} (\log \det [\mathbf{K}_{\theta p}]). \quad (36)$$

where  $\Delta x_{\min}$  is the extension of the chain in the ground state without thermal fluctuation. Here we have used the facts that  $L_0 - \partial E_{\min} / \partial (l_0 \tau_N) = \Delta x_{\min}$ , and also that the stiffness matrix  $[\mathbf{K}_\varepsilon]$  does not depend on the distributed loads  $\tau$ . We note that the last term in Eq. 36, which is proportional to the thermal energy  $k_B T$ , is the contribution of the average extension from thermal fluctuation. When  $T = 0$  and there is no thermal fluctuation,  $\langle \Delta x \rangle = \Delta x_{\min}$ , as it should be, because the only configuration sampled is the minimum energy state.

### 2.5 Thermal fluctuation around the ground state

For the quantities that do not have clear conjugate pairs, their fluctuations can be evaluated directly from a Boltzmann weighted sum. The key is to use the following multi-dimensional Gaussian integral formula [16]:

$$\langle f(\vec{x}) \rangle = \frac{\int f(\vec{x}) \cdot \exp\left(-\frac{1}{2} \vec{x}^T \cdot [\mathbf{A}] \vec{x}\right) d\vec{x}}{\int \exp\left(-\frac{1}{2} \vec{x}^T \cdot [\mathbf{A}] \vec{x}\right) d\vec{x}} = \exp\left(\frac{1}{2} \sum_{i,j=1}^N [\mathbf{A}]_{ij}^{-1} \frac{\partial}{\partial x_i} \frac{\partial}{\partial x_j}\right) f(\vec{x}) \Big|_{\vec{x}=\vec{0}}. \quad (37)$$

Here  $f(\vec{x})$  can be some general polynomial functions which are weighted by the Boltzmann factor in the numerator. The denominator on the left-hand-side is just the partition function, which serves as the normalization factor to the weighted average. On the right-hand-side, the exponential operating on the differential operator is understood as a power series:  $\exp(a) = 1 + a + a^2/2 + \dots$ .

Using Eq. 37, the thermal fluctuation in strain can be evaluated. In particular, for the strain  $\varepsilon$ , the mean deviation and mean square deviation from the ground state are respectively:

$$\langle \Delta \varepsilon_i \rangle = 0 \quad (38)$$

$$\langle \Delta \varepsilon_i \cdot \Delta \varepsilon_j \rangle = k_B T [\mathbf{K}_\varepsilon]_{ij}^{-1} = \frac{\delta_{ij} k_B T}{K_{si} l_0}. \quad (39)$$

Similarly, the fluctuation in the angles  $\vec{\theta}$  is:

$$\langle \Delta \theta_i \rangle = 0 \quad (40)$$

$$\langle \Delta \theta_i \cdot \Delta \theta_j \rangle = k_B T [\mathbf{K}_{\theta p}]_{ij}^{-1}. \quad (41)$$

We see that the mean square thermal fluctuations around the ground state increase linearly as we increase the temperature, and decrease as the we increase the mechanical stiffness of the system, in agreement with intuition.

In experiments one typically measures the fluctuations in displacements. These can be calculated directly from Eq. 37, or alternatively, using Eq. 39 and 41. In particular, the fluctuation in the transverse displacement is:

$$\langle \Delta w_i \rangle = l_0 \sum_{m=1}^i \langle \theta_m \rangle = 0, \quad (42)$$

$$\langle \Delta w_i \cdot \Delta w_j \rangle = l_0^2 \sum_{m=1}^i \sum_{n=1}^j \langle \Delta \theta_m \cdot \Delta \theta_n \rangle. \quad (43)$$

Similarly, the fluctuation in displacement  $u$  can be obtained by using the fourth moment of the multi-dimensional Gaussian distribution:

$$\langle \Delta u_i \rangle = -\frac{l_0}{2} \sum_{m=1}^i \langle \theta_m^2 \rangle, \quad (44)$$

$$\langle \Delta u_i^2 \rangle = k_B T l_0 \sum_{m=1}^i \frac{1}{K_{sm}} \quad (45)$$

$$+ \frac{l_0^2}{4} \sum_{m=1}^i \sum_{n=1}^i \left( \langle \Delta \theta_m^2 \rangle \langle \Delta \theta_n^2 \rangle + 2 \langle \Delta \theta_m \cdot \Delta \theta_n \rangle^2 + 4 \bar{\theta}_m \bar{\theta}_n \langle \Delta \theta_m \cdot \Delta \theta_n \rangle \right). \quad (46)$$

Here  $\bar{\theta}$  is the angle for the ground state configuration. We note that while  $\langle \Delta w_i \cdot \Delta w_j \rangle$  is the fluctuation around the ground state,  $\langle \Delta u_i \cdot \Delta u_j \rangle$  is not; because  $\langle \Delta w_i \rangle = 0$  and  $\langle \Delta u_i \rangle$  is not.

### 3 Results

We first show in Fig. 2 that the theories for a continuous rod and the theory for a discrete chain yield the same result when  $\tau$  is a constant along the arc length. For large  $\tau$ , the thermal fluctuations are already stretched out, so that the force-extension curve is almost linear, due to elastic stretching.

We next focus on the results from the discrete model and compare the behavior of a chain under distributed force and end-to-end force. Average end-to-end extension of the semi-flexible chain  $\langle \Delta x \rangle$  versus  $\tau$  is plotted again in Fig. 3 in red solid line. If we turn off the thermal fluctuations, the chain behaves just as a linear elastic rod and the force-extension relation is shown in red dashed line in the same figure. To make a comparison, we apply a point force  $F$  at the end of the chain. Under the same net force:  $F = \tau L_0$ , the chain under end-to-end force suffers larger extension

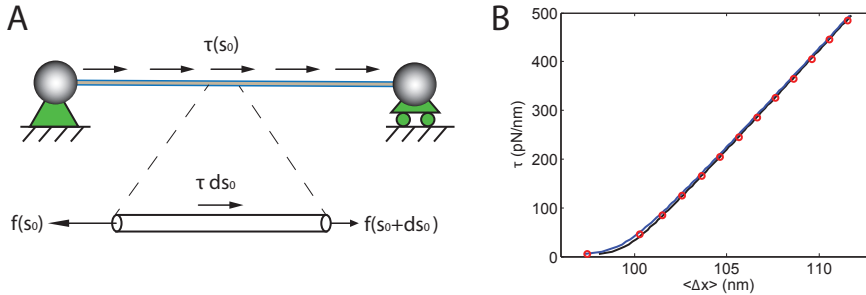


Figure 2: Comparison between the continuous models and the discrete model. (A) Force balance for an infinitesimal segment of a continuous rod. (B) Comparison of the results for a continuous rod (Black curve: Fourier series method and Eq. 15; Blue (almost overlaps with the black curve): method using force balance on infinitesimal segment and Eq. 20) and a discrete chain (red circles). The filament is under constant  $\tau$  along the arc length so that Fourier series method can be applied. Here a 100nm chain is discretized into 1000 segments. The results match quite well.

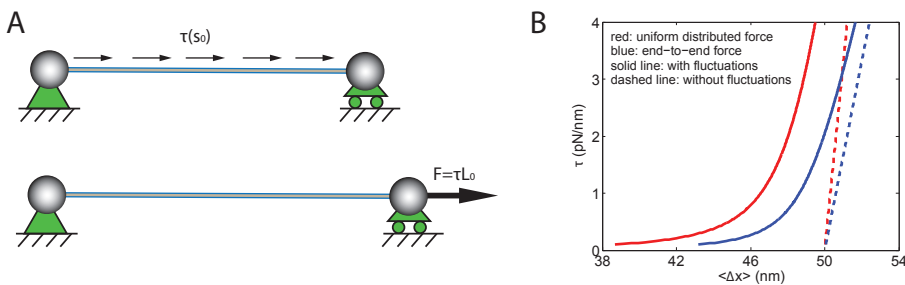


Figure 3: Force-extension relations for a wormlike chain (1: red solid line) under uniform distributed load  $\tau$  with thermal fluctuations, (2: red dashed line) under uniform distributed load  $\tau$  without thermal fluctuations, (3: blue solid line) under end-to-end force  $F = \tau L_0$  with thermal fluctuations, and (4: blue dashed line) under end-to-end force without thermal fluctuations. The reference contour length of the chain is  $L_0 = 50\text{nm}$ . The persistence length is 5nm. The segment length is 0.5nm with  $N = 100$  segments.

(Fig. 3 blue) than the one under distributed load. This is in agreement with result from the Fourier series method for a continuous rod, which tells us the effective end-to-end force for a distributed load is  $\tau L_0/2$ , instead of  $\tau L_0$ . Another way to understand this result is by doing force balance on the chain. Under end-to-end applied force, the stress along the chain is uniform:  $\sigma \equiv F/A = \tau L_0/A$ , where  $A$  is the cross sectional area of the chain. Under distributed force, on the other hand, the stress along the chain varies linearly  $\sigma = \tau(L_0 - s_0)/A$ , and it is smaller than the stress in the previous case everywhere except at  $s_0 = 0$ . Therefore, it is not surprising that a chain under end-to-end force suffers larger extension.

The fact that uniform distributed  $\tau$  causes less internal tension in the chain than the end-to-end force  $F = \tau L_0$  is also reflected in the transverse fluctuation profile (Fig. 4). Because internal tension stiffens the filament, a chain with less internal tension is expected to have larger thermal fluctuation. Indeed, our result shows that the magnitude of transverse fluctuation is significantly larger for a chain under uniform distributed force. Moreover, unlike the end-to-end force case, internal tension is not a constant along the arc length when the chain is subjected to uniform  $\tau$ ; therefore, the transverse fluctuation profile is not symmetric. The end of the chain with less internal force has more fluctuations, as shown in Fig. 4.

Next, as a practical application of our methods, we analyze the stretching and fluctuations of a piece of DNA in a linear microfluidic channel and a constant-strain-rate channel, both of which have been fabricated in experiments [15]. For a linear channel, the channel width varies as  $w(x) = ax + b$ , where  $a$  and  $b$  are two constants. On the other hand, a constant-strain-rate channel has a shape  $w(x) = a/(1 + x/b)$  (Fig. 5A). Since the fluid velocity is inversely proportional to the channel width  $w$ , a polymer confined in the channel experiences drag force  $\tau = d_t v(x)$  that varies along its arc length. Here  $d_t$  is the drag coefficient per unit length and it is set to  $d_t = 1.2\text{pN} \cdot \text{ms} \cdot \mu\text{m}^{-2}$  [15] in our calculation. Fig. 5B and C show respectively the extension and fluctuations of the polymer in fluid flow. With the same entrance width (width on the leftmost side) and exit width (width on the rightmost side), a constant-strain-rate channel is narrower in most of its middle region compared to a linear channel. Therefore, a polymer suffers larger drag force and less transverse fluctuations in a constant-strain-rate channel. This leads to a larger end-to-end extension. In Fig. 5C, we also compare the fluctuations of a hinged-hinged polymer (dashed line) and a hinged-free polymer, whose right end is not constrained on the  $x$  axis. The fluctuation for the hinged-free polymer is larger than that for the hinged-hinged polymer, as expected. In this study, we neglect the entropic force due to the non-uniform channel width.

Finally, in Fig. 6, we show the transverse fluctuation of a chain subjected to uniform  $\tau$  plus a point load in the middle. The figure shows that the point load stretches the

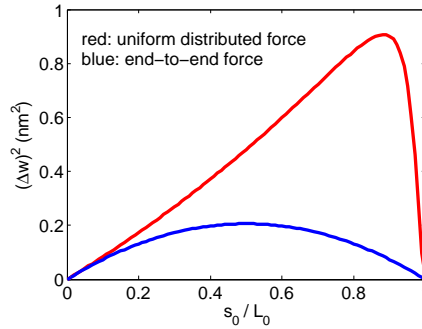


Figure 4: Transverse fluctuation of a chain under uniform distributed  $\tau = 5\text{ pN}/\text{nm}$  (red), and under end-to-end applied force  $F = \tau L_0$  (blue). Under distributed force, the chain has larger thermal fluctuations with an asymmetric fluctuation profile.

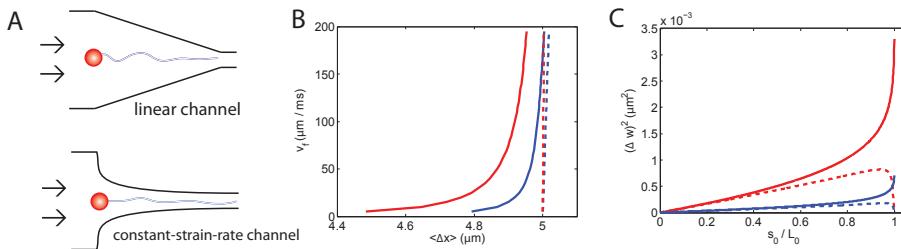


Figure 5: DNA in non-uniform microfluidic channels. (A) A piece of DNA confined in a linear channel and a constant-strain rate channel. Both channel types have been fabricated in experiments [15]. (B) The velocity in the non-uniform channel is inversely proportional to the channel width. Therefore, given the velocity  $v_f$  at the exit (rightmost) end, the entire velocity profile inside the channel is known, which then leads to the drag force  $\tau = d_t v$  along the polymer. Here the end-to-end extension of the polymer is plotted against  $v_f$ . As we increase the flow velocity, the strain along polymer increases, resulting in a larger end-to-end extension. Red: DNA in a linear channel. Blue: DNA in a constant-strain-rate channel. Dashed/Solid lines: extension with/without the contribution of thermal fluctuations. (C) Transverse fluctuations along the polymer arc length. Red and blue for DNA in a linear and a constant-strain-rate channel respectively. Solid line is for a DNA with one end hinged and the other end free to fluctuate. Dashed line is for the same DNA with both ends hinged on the  $x$  axis.

left half of the chain and reduces the fluctuation there.

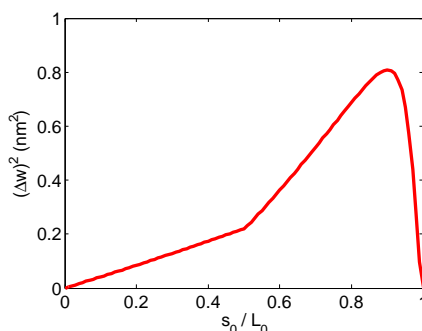


Figure 6: Transverse fluctuation of a chain under uniform distributed  $\tau$  plus a point load  $F$  in the middle. The left half of the chain has less fluctuation because the stretching of the point loads reduces the thermal fluctuations.

#### 4 Conclusions

We analyze the thermoelastic behavior of a fluctuating elastic filament under distributed loads in this paper. We obtain, by means of a Fourier analysis on a continuous filament, analytic results when the polymer is under uniform distributed load. We find that a filament under uniform distributed load  $\tau$  per unit reference length can be viewed as one under an effective end-to-end force of  $\tau L_0/2$  if we are only interested in the force-extension relation. However, to get the fluctuations of a filament under general loadings, we need to first discretize the filament and approximate the path integral for the partition function as a multi-dimensional Gaussian integral. Once the partition function is calculated, all other quantities can be obtained by differentiation using standard thermodynamic techniques. As an illustration, we apply our methods to DNA under non-uniform distributed loads as is the case for DNA stretched by flow fields in microfluidic channels.

**Acknowledgement:** We acknowledge partial support from an NSF CAREER award to PKP through grant number NSF CMMI-0953548.

#### References

1. Bustamante C, Marko JF, Siggia ED, Smith S. 1994. **Entropic elasticity of lambda-phage DNA.** *Science* 265:1599-1600.
2. Marko JF, Siggia ED. 1995. **Stretching DNA.** *Macromolecules* 28:8759-8770.



3. Odijk T. 1995. **Stiff chains and filaments under tension.** *Macromolecules*. 28:7016-7018.
4. Nelson P. 2008. **Biological Physics: Energy, Information, Life.** updated first ed. W. H. Freeman and Company, New York.
5. Purohit PK, Arsenault ME, Goldman Y, Bau HH. 2008. **The mechanics of short rod-like molecules in tension.** *Int. J. Non-linear Mech.* 43(10):1056-1063.
6. Arsenault ME, Purohit PK, Goldman YE, Shuman H, Bau HH. 2010. **Comparison of brownian-dynamics-based estimates of polymer tension with direct force measurements.** *Phys. Rev. E* 82:051923.
7. Su T, Purohit, PK. 2010. **Thermomechanics of a heterogeneous fluctuating chain** *J. Mech. Phys. Solids*. 58:164-186.
8. Larson RG, Perkins TT, Smith DE, Chu S. 1996. **Hydrodynamics of a DNA molecule in a flow field.** *Phys. Rev. E* 55:1794-1797.
9. Phillips R. 2008. **Physical Biology of the Cell.** Garland Science.
10. Wang J, Gao H. 2007. **Stretching a stiff polymer in a tube.** *J. Mater. Sci.* 42:8838-8843.
11. Maier B, Seifert U, Rädler JO. 2002. **Elastic response of DNA to external electric fields in two dimensions.** *Europhysics Letters* 60:622-628.
12. Benetatos P, Frey E. 2004. **Linear response of a grafted semiflexible polymer to a uniform force field.** *Phys. Rev. E* 70, 051806.
13. Hori Y, Prasad A, Kondev J. 2007. **Stretching short biopolymers by fields and forces.** *Phys. Rev. E* 75, 041904.
14. Zhang YL, Crothers DM. 2003. **Statistical mechanics of sequence-dependent circular DNA and its application for DNA cyclization.** *Biophys. J.* 84:136-153.
15. Larson JW, Yantz GR, Zhong Q, Charnas R, D'Antoni CM, Gallo MV, Gillis KA, Neely LA, Phillips KM, Wong GG, Gullans SR, Gilmanshin R. 2006. **Single DNA molecule stretching in sudden mixed shear and elongational microflows.** *Lab Chip*. 6:1187-1199.
16. Chirikjian GS. 2009. **Stochastic models, information theory, and Lie groups.** Birkhauser.

